Journal of Food Measurement and Characterization (2023) 17:5550–5568
https://doi.org/10.1007/s11694-023-02062-9

ORIGINAL PAPER

Montmorillonite and chitosan modulates the techno-functional, mechanical, antibacterial, biodegradation and morphological characteristics of gluten-based nanocomposite films

Tamanna Sharma[1] · Gurkirat Kaur[2] · Arashdeep Singh[1] · Prastuty Singh[1]

Received: 26 April 2023 / Accepted: 11 July 2023 / Published online: 23 July 2023

Abstract

The main objective of this work was to prepare biodegradable packaging film based on the organic base polymer for the replacement of petroleum based plastic films. Therefore, the present investigation is conducted to characterize gluten-polyvinyl alcohol (PVA) based bionanocomposite films containing two concentrations of montmorillonite (MMT) as 2% and 4% and chitosan as 1.5% and 2.5% for their functional properties, barrier properties, morphological, biodegradable, and microbial properties. Results indicated that films prepared with 2% MMT and 2.5% chitosan has represented high transparency with low opacity value (2.47 $AUmm^{-1}$). Further, tensile strength (TS) and water vapour transmission rate (WVTR) of the films were found higher in the same film as 58.94 MPa and 0.06 g/h cm^2, respectively. However, uniform and smooth surface morphology was obtained due to the interaction between MMT (2%) and matrix. While, increasing the concentration of MMT cause cavities on the surface of films and reduced TS of the films. The composite films degraded under soil within 55 days as noticeable achievement in research area. Moreover, intercalation between gluten-PVA matrix and MMT resulted in appreciable modifications of their structures, which were supported by X-ray diffraction (XRD) and Fourier transform infrared (FT-IR) spectroscopy. The nanoclay exfoliates for better interaction with other components and large surface area make their functionality more intense in comparison to macromolecules. Therefore, the synergistic effect of MMT and chitosan has enhanced functional, mechanical and barrier characteristics, can be an alternative approach for the replacement of hazardous non-biodegradable plastic packaging material being used for industrial applications.

✉ Tamanna Sharma
tamanna96sharma@gmail.com

✉ Arashdeep Singh
arash.pau@gmail.com

Gurkirat Kaur
kgurkirat25@gmail.com

Prastuty Singh
15prastuty@gmail.com

[1] Department of Food Science and Technology, Punjab Agricultural University, Ludhiana, Punjab 141004, India

[2] Electron Microscopy and Nanoscience Lab, Punjab Agricultural University, Ludhiana, Punjab 141004, India

Graphical abstract

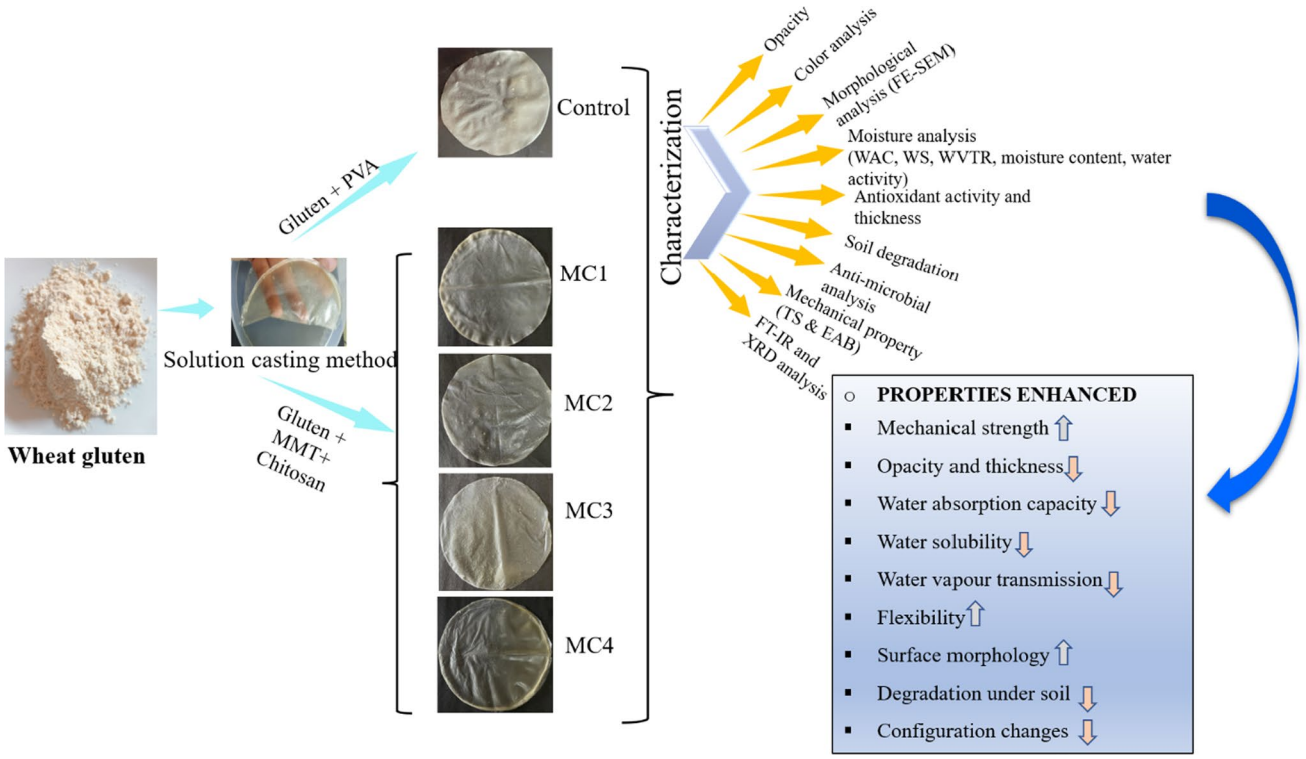

Keywords Biodegradable · Bionanocomposite · Chitosan · Gluten · Montmorillonite · Polyvinyl alcohol

Introduction

Plastics are employed extensively in daily human activities like the food business, grocery stores, and the transportation of products. Plastics are produced from petrochemical-based polymers, such as polyethylene (PE), polyvinyl chloride (PVC), and polyethylene terephthalate (PET) which are valued for their affordability and good thermal and mechanical properties [1]. The used plastic packaging material and its subsequent random disposal on the earth generate serious health and environmental problems [2]. To overcome such problems customer and environmental legislation demands *green polymeric material* for the development of packaging material in the replacement of plastic [2]. These materials would be made of natural resources and perhaps be biodegradable. The terms "biodegradable polymers" and "biopolymers" describe polymeric materials that can degrade due to the enzymatic activity of microorganisms such as bacteria, fungi, and algae in a bioactive environment [1]. Although employing biodegradable polymers in packaging is crucial, the cost of this technology makes it unaffordable from this perspective. As a result, the different countries prioritize on finding substitutes or solutions to lessen this environmental issue. In this regard, numerous studies have focused on the use of proteins, particularly wheat gluten, for packaging purposes. In addition, the proteins exert stretchable and interactive nature towards other components in the blend that could be an important organic base for film formation [3]. Wheat gluten is a vital agropolymer that consists of two components i.e., glutenin (soluble in acids) and gliadin (soluble in 70% alcohol). Further, the presence of glutenin and gliadin fractions effective oil and gas barrier properties in produced films [1]. There are primarily two causes for this favorable gas barrier behavior i.e., low polarity of gases and the presence of crystalline domains causes these gases to have low solubilities, weak interactions, and consequently low gas permeabilities [4]. The primary disadvantage is high water sensitivity that weakens the mechanical and barrier properties of films. In addition, polyvinyl alcohol (PVA) is a biodegradable water-soluble polymer that provides strength and flexibility to the films [5].

In addition, the solution casting method is considered as a convenient and low-cost method which was used to develop highly transparent and uniform films in comparison

to compression molding and extrusion method [5]. The PVA polymer is well known for its low cost and effective gas barrier properties. PVA has been authorized for use as a coating on dietary supplements that are intended for human consumption [4]. It is well known that PVA has excellent gas barrier qualities. PVA and gluten polypeptides cross-links through intermolecular hydrophobic interaction, provoking stronger tensile strength (TS) and lower elongation at break (EAB) [6]. Additionally, PVA and gluten have synergistic effect on gas barrier properties by following two factors i.e., low polarity of gases and crystalline domains cause poor gas solubility/permeability which also results in weak interactions [1]. Some studies were conducted which showed the combination of PVA and gluten has stronger hydrogen bonding with each other as well as nanoparticles which can reduce the film crystallinity and degradation [7]. Further, nanofillers devoted an important role for high transparency and mechanical properties due to the large surface area to volume ratio. A natural nanofillers such as montmorillonite (MMT) is a layered silicate with a negative surface charge in which a central octahedral sheet of alumina or magnesia connected to two exterior silica tetrahedrons forms the ideal crystalline structure of layered silicates, which are composed of two-dimensional layers [6]. MMT can be exfoliated in water to create anionic platelets that are 1 nm thick and have other two dimensions between 150 to 200 nm [4]. Basically, the exfoliated nanoparticles effectively interact with another polymer matrix, results high TS, high-temperature resistance and low density to the films. These mechanical and thermal properties can recommend such ingredients for the desirable final film comparable with the functional properties of plastic films [6]. Many researchers have reported that the produced nanocomposite had a high degree of transparency, which is preferentially advantageous in many applications in the food packaging sector [2, 4, 6]. By the reference of many scientific studies, the main purpose of incorporation of MMT in the formulation is to employ better tensile modulus, good barrier properties, higher thermal stability, and reduction in the aging rate of gluten films. Furthermore, MMT is responsible for highly transparent nanocomposite films, and prospective applications in a variety of industries, such as electronics, medicinal applications, and food packaging.

Chitosan is created by deacetylating chitin, which is composed of unbranched chains of β-(1,4)2-acetoamido-2-deoxy-D-glucose. Furthermore, chitosan is recognized to have effective antifungal and antibacterial activities. It possesses antibacterial properties against *Escherichia coli, Staphylococcus aureus, Listeria monocytogens,* etc., by the formation of dense polymer film on the outer surface of the microbial cell and retards nutrient exchange, leading to bacterial death [8]. Chitosan has many applications due to its higher concentration of chelating amino groups. Besides this, chitosan has several outstanding benefits, including biodegradability, biocompatibility, low toxicity, and bioactivity [9]. According to several studies, adding chitosan and nanofiller to composite materials can increase their TS, storage modulus, glass transition temperature, and water vapor permeability while lowering their EAB [8]. Lai et al. [10] have investigated the excellent compatibility of montmorillonite and chitosan, which leads to high elongation at break, thermal and structural improvement. The consideration of film forming network of gluten and PVA, strength and barrier making property of MMT, antibacterial and uniformity generating property of chitosan could lead to development of highly appreciable blend for film formation with greater, biodegradability, transparency and uniformity in morphological aspects [11–13]. The related studies employed convenient disposal, sustainability and versatility, which can make it cost-effective globally and packaging industries can adapt this technology for product stability and survivability through the supply chain to provide higher quality to their customers [2]. The main objective of this research work is to develop and characterize gluten-based bionanocomposite packaging films using various MMT concentrations and observing the effects of chitosan. This work was related to assessing how the integration of nano clay-chitosan and PVA influenced the functionality of gluten-based films through the analysis of various physical, mechanical, and structural aspects of the produced films. Further, the microstructure and physiological examination of this composite system were elaborated in relation to moisture solubility, moisture transmission, thermal stability, mechanical strength, water barrier and biodegradability.

Materials and methods

Wheat gluten powder (95% pure) was procured from Istore Direct trading LLP (Mumbai), glycerol (Molychem, India) was added for plasticity and MMT (Himedia, GRM4750-250G) was used as nanofiller. PVA as network forming intercalating polymer was purchased from Isochem Laboratories Angamaly, Kochi. Chitosan (Bangalore Fine Chem, Bangalore-60) was used in two concentrations to determine antimicrobial efficiency in the films. Ethanol, acetic acid and sodium hydroxide (NaOH) were purchased from FTC, India (Ghaziabad, UP) and used as solvents for the preparation of gluten slurry. *Escherichia coli* (ATCC 4157-433P), *Staphylococcus aureus* (ATCC 11632-0462P), Tryptone soy broth and Mueller–Hinton agar were purchased from Himedia, Mumbai.

Preparation of blends

The known weight (5% w/v) of PVA powder was dissolved in 30 mL of distilled water and homogenized by a

magnetic stirrer at 80 °C for 120 min until clear solution was obtained. The predetermined speed of the magnetic stirrer was 700 rpm. Further, two concentrations of chitosan i.e., 1.5% w/v and 2.5% w/v were weighed and dissolved in 10 mL of 1% w/v of acetic acid and 10 mL distilled water, individually. The solution was mixed on a magnetic stirrer under ambient conditions at 1000 rpm for 2.5 h [14]. Both solutions can be preserved in conical flasks separately for further use (Fig. 1).

Preparation of MMT solution

The detailed process of preparation of MMT solution at the nanoscale was depicted in Fig. 1. MMT solution was developed by disseminating 2.0% w/v and 4.0% w/v of MMT powder in distilled water. The mixture was homogenized continuously with a magnetic stirrer (600 rpm) for 6 h at 45 °C. The collected suspensions were centrifuged for 15 min at 3000 rpm. Further, the supernatant was collected for the preparation of film formulations [13].

Film development

Wheat gluten/MMT/chitosan blend films were developed from gluten solution that is dissolved with 30 mL of 70% ethanol and 5 mL of 1.5% acetic acid solution [12]. The prepared blend of PVA was added to the gluten solution with continuous stirring at 700 rpm. Then, different nanocomposite film dispersions were prepared with two concentrations of MMT (2.0% v/v and 4.0% v/v) and chitosan (1.5% v/v and 2.5% v/v), added into the previous solution of gluten and PVA. In the same solution, 5.0% v/v glycerol was dissolved as a plasticizer. The temperature of this dispersion should not exceed 80 °C, otherwise, disintegration of the solution occurs and no uniformity was obtained beyond this point. Then the alkaline pH of the whole solution should be maintained at 10 by the addition of 0.1N NaOH solution. Further, air bubbles were removed by ultrasonication (4 min) and the slurry temperature was reduced up to 35 °C. Afterward, equal volume (22 mL) of the cooled suspension was cast onto petri plates (diameter = 15 cm) and left in the hot air oven for 15 min at 55 °C. Prepared dried films were peeled off and stored in an airtight container at ambient temperature (25 ± 2 °C) [14]. The preparation of nanocomposite gluten/MMT/chitosan was illustrated in Fig. 1. Abbreviations used for developed film samples were: (a) Control for a film with no MMT or chitosan; (b) MC1 containing gluten along with MMT and chitosan of 2% and 1.5%, respectively; (c) MC2 containing gluten along with MMT and chitosan of 2% and 2.5%, respectively; (d) MC3 containing gluten along with MMT and chitosan of 4% and 1.5%, respectively; (e) MC4 containing gluten along with MMT and chitosan of 4% and 2.5%, respectively (Fig. 2).

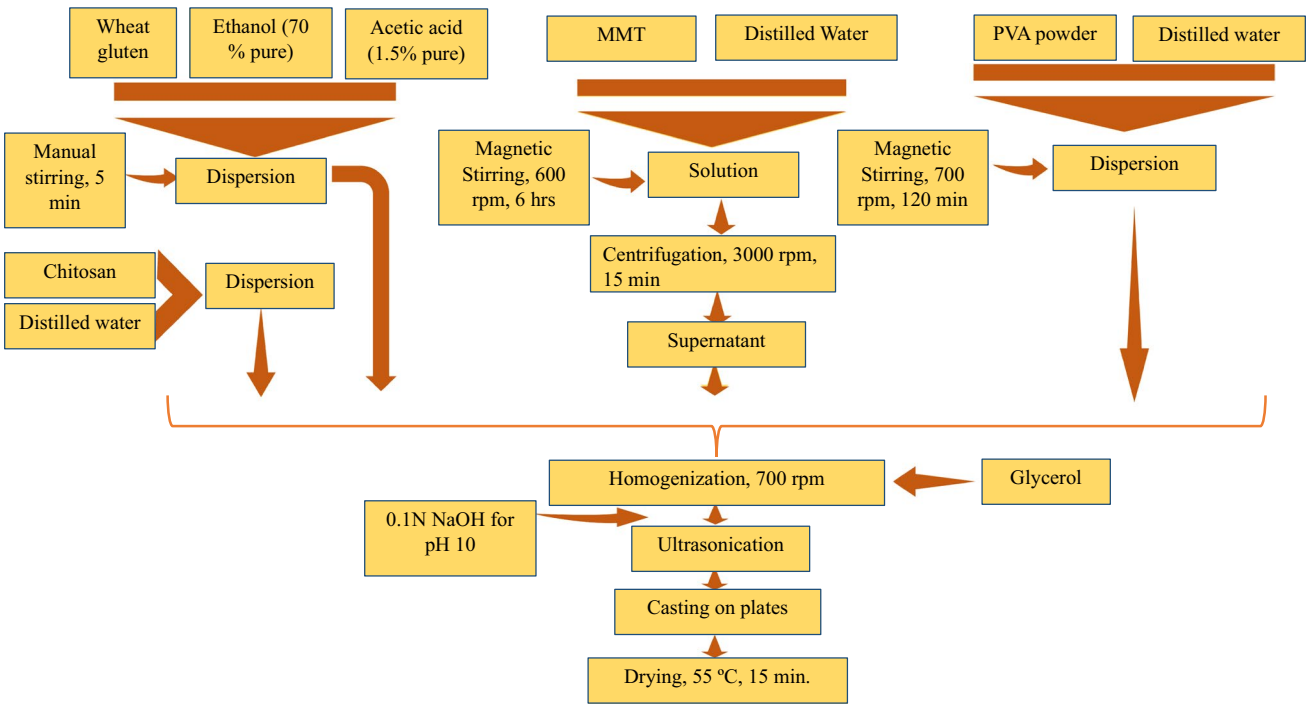

Fig. 1 Schematic illustration of preparation methodology of gluten based bionanocomposite films

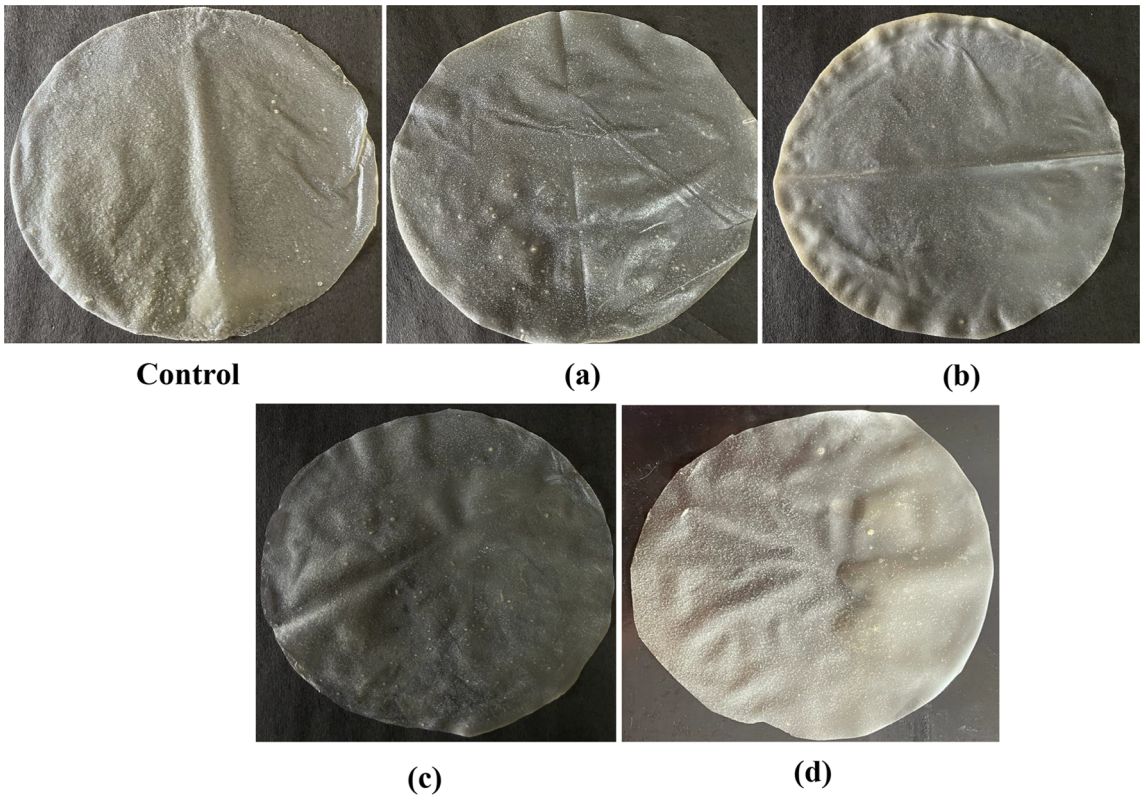

Fig. 2 Pictorial representation of gluten protein based bionanocomposite films; Control (gluten), **a** gluten/MMT-2%/chitosan 1.5% (MC1), **b** gluten/MMT-2%/chitosan 2.5% (MC2) **c** gluten/MMT-4%/chitosan 1.5% (MC3) **d** gluten/MMT-4%/chitosan 2.5% (MC4)

Characterization of nanocomposite films

Moisture content, water activity and thickness

The gravimetric method was used to determine the free moisture content of the film, and samples of the film were dried for 24 h at 105 ± 2 °C. For each sample, the test was carried out in triplicates [15]. On the other hand, water activity was also measured with an Aqua lab (Decagon, USA) water activity meter at 21 °C according to Benbettaieb et al. [16]. A portable handheld micrometer (Mitutoyo-Absolute digital, Japan) with a precision of 0.001 mm was utilized to estimate the thickness of gluten-based films. The readings were in triplicates from all the directions of the film to confirm uniformity [15].

Mechanical properties

Mechanical properties such as TS and EAB of nanocomposite films were examined by texture analyzer (Stable Micro Systems, Model: TA.TXT. Plus). T_s and E_b were measured by cutting the films in a rectangular shape having dimensions of 6 cm × 3 cm × 0.12 mm. The grip separation of 5 cm had 5/ms of cross-sectional speed and 50% of the strain value was used to perform the analysis [13]. The following formula was used to determine TS (1) and EAB (2);

$$TS = \frac{F_{max}}{A} \quad (1)$$

where F_{max} (MPa) is the highest load required for bursting of film and A is the area (m^2) of test film.

$$EAB = \frac{L}{L_0} \times 100 \quad (2)$$

where, L is the length difference after elongation, while L_0 is the initial length of the test film.

Morphological analysis

The surface characteristics of produced film were obtained in pictorial form by using field emission scanning electron microscopy (FE-SEM) (Joel, JSM-7610 F Plus, Tokyo, Japan) with a 10 µm scale, accelerating voltage of 5.0 kV and working distance of 8.0 mm. The film samples were cut manually and mounted on a stub with gold sputter coating for high conductivity. Prepared samples were exposed

to a predefined accelerating electron load with 8.0 mA of current.

X-ray diffraction (XRD) analysis

The dispersion condition of the nanoparticles in the gluten matrix is determined by X-ray photoelectron spectroscopy (X'Pert Pro XRD Diffractometer). X-rays were used to determine the crystallinity and molecular miscibility of films. Film samples were cut in the form of strips having dimensions of 0.1 cm × 0.1 cm. The XRD patterns were developed with an angular range (2Θ) of 5-60° at a voltage of 45 kV and a scan step time of 30 s. For the detection of X-Ray diffraction x' Celerator solid-state detector was used. The X-Ray diffractogram was derived in 2Θ position (X-axis) versus intensity (Y-axis).

Fourier transform infrared (FT-IR) analysis

FT-IR graphical spectra of bionanocomposite films were obtained by using the model Agilent Cary 630 FT-IR to determine the influence of MMT and chitosan in the gluten film formulations. Samples were directly placed on the ATR (attenuated total reflectance) crystal after background clearance with methanol. The wavenumber region of the samples was 4000–750 cm^{-1} range.

Color

Color analysis of the nanocomposite films was determined by Hunter lab colorimeter (Colorex, EZ-45/0-LAV, USA). The chromacity parameters (a and b*) and brightness (L*) of the film were determined at three randomly chosen spots on the film surface. The standard white plate was used for calibration of the instrument, and ΔE (total color difference) was calculated according to Eq. (3):

$$\Delta E^* = \sqrt{(\Delta L^*)^2 + (\Delta a^*)^2 + (\Delta b^*)^2} \tag{3}$$

Opacity

Films were cut in square shapes (2 cm × 2 cm) for defining their opacity by placing them in the spectrophotometer cuvettes. The wavelength range of spectrophotometer (Model, SANCO-SAN-722) for each sample was set at 400 to 800 nm. The transmittance was measured using an empty reference test cell at 600 nm wavelength. The opacity of nanocomposite films was assessed using the following formula given in Eq. (4):

$$\text{Opacity} = \frac{A_{600}}{x} \tag{4}$$

where A_{600} represents the absorbance at wavelength 600 nm and x is the thickness of the film in mm [17].

Antioxidant activity

The antioxidant activity of nanocomposite films was measured as per the method of Kadam et al. [18]. 2,2-Diphenyl-l-picrylhydrazyl (DPPH) was used as a source of free radicals. The known area of films (3 cm^2) was noted and mixed in 10 mL of distilled water. Afterward, centrifugation was done at 500 rpm and 1 mL of supernatant was collected. A quantity of 3.9 mL of 610–5 mol/L DPPH in methanol was put in a cuvette with 0.1 mL of sample extracted and a decrease in absorbance was measured at 517 nm for 30 min or until the absorbance became steady. Methanol was used as a blank. The remaining DPPH concentration was calculated using the following Eq. (5):

$$\text{Antioxidant activity}(\%\ \text{DPPH scavenging assay}) = \frac{A_{\text{control}} - A_{\text{sample}}}{A_{\text{control}}} \times 100 \tag{5}$$

where $A_{control}$ is the absorbance of control and A_{sample} is the absorbance of sample.

Water solubility (WS)

The technique described by Kariminejad et al. [19]. was used to measure the film's solubility in water. The percentage of the film's dry matter that was dissolved after 24 h, was used to calculate the film's water solubility. Initially, all the samples were cut (4 cm × 2 cm) and placed in a desiccator with silica pouches to acquire initial dry matter weight (W_i). Afterward, samples were submerged in distilled water (50 mL) at ambient temperature (25 °C). Then centrifugation (3000×*g* for 5 min) is done to separate insoluble residue. The final weight (W_f) of the leftover was obtained by drying in a hot air oven at 60 °C. The following formula in Eq. (6) was used to calculate the solubility of films in water (WS%).

$$\text{WS}(\%) = W_i - \frac{W_f}{W_i} \times 100 \tag{6}$$

Water vapor transmission rate (WVTR)

WVTR has been determined by using the desiccant method. The small beakers were filled with silica gel, having the property of desiccant. Further, test films were used to tightly cover the mouth of beakers with para film sealant and the resulting constituents were weighed. Then sealed beakers were kept inside a hermetic desiccator, and had saturated NaCl solution (72.0 ± 2% RH) at the bottom for 24 h. The beakers were then weighed at regular intervals after every 6 h to perform a water loss analysis. The weight slope was then calculated from the obtained data using a linear regression equation. The following Eq. (7) was used to compute the WVTR of composite films [13]:

$$\mathrm{WVTR}\left(\mathrm{g/hcm^2}\right) = \frac{M_v}{A} \tag{7}$$

where M_v equals to the slope of cup weight (g/h) and A is an area of the test film (cm^2).

Water absorption capacity (WAC)

The composite films were cut into known dimensions (1.5 cm × 1.5 cm) and placed inside a hermetic desiccator with silica gel to get a moisture free sample for the time of 5 days. Further, samples were dipped in 30 mL distilled water for 45 min to get the final weight of the swollen films. The absorbed water was measured as WAC of test films and the formula is given below in Eq. (8) [3]:

$$\mathrm{WAC}(\%) = M_t - \frac{M_0}{M_0} \times 100 \tag{8}$$

where W_i and W_f are the initial and final weights of the nanocomposite films, respectively.

Soil burial test

Soil burial test is used to determine the biodegradability of bionanocomposite films 5 cm below the conditioned soil as described by Gujral et al. [20] under minor modifications. Films were cut into 3 cm × 2 cm and the weight loss was observed over the time of 54 days. The initial weight of all the test films was observed initially and then weighed after 7 days of regular intervals. After a week, the samples of the film were taken out and the soil that had adhered to the film's surface was removed properly. The following formula in Eq. (9) was used to determine biodegradability of films:

$$\mathrm{Degradation\ of\ films}(\%\ \mathrm{weight\ loss}) = \frac{W_i - W_d}{W_i} \times 100 \tag{9}$$

where W_i is the initial weight of the film, while W_d is the weight of the degraded film.

Antimicrobial analysis

The disc diffusion method was used for analyzing the antimicrobial activity of the prepared nanocomposite films against microbial cultures of *Staphylococcus aureus* (MTCC no 096) and *Escherichia coli* (MTCC no 443). The frozen cultures were regenerated by dissolving 100 mL of bacterial culture to 10 mL of tryptone soy broth and placed in an incubate for 24 h at 37 °C. Now bacterial broth of 0.1 mL was poured over the surface of the agar (Gujarat general food chemical Pvt Ltd). The sample were cut into disc form (4 mm diameter) and were placed over the solidified agar media which is previously inoculated. Put the plates inside the incubator at 37 °C for 24 h. The zone of inhibition was developed and measured by a caliper which indicated the antimicrobial activity of the films against the microbial load [13].

Statistical analysis

All the parameters and their comparisons were done using ANOVA and Duncan's post hoc tests at a 5% level of significance. A statistical study was carried out in triplicates for demonstrating the mean value and standard deviation by using IBM SPSS Statistics 20.

Result and discussion

Moisture content, water activity and thickness

The moisture and water activity values are illustrated in Table 1. The moisture content significantly decreases ($p \leq 0.05$) in the nanocomposite films with increase in the concentration of MMT (2–4%) and chitosan (1.5–2.5%) in the sample MC1 to MC4. Whereas, the control sample represents a high amount of moisture content as 16.85%. The explanation for the decrease in moisture content may be the interfacial contact (electrostatic and hydrogen bonding) between MMT and gluten, which results in the intercalation of gluten inside the galleries of MMT and the compactness of the film [21]. Similarly, water activity has been analyzed as the concentration of free water also decreased from 0.55 (control) to 0.26 (MC3). The multilayer matrix of the films does not allow free water to flow within the galleries [22].

The thickness of 0.10 and 0.33 was significantly ($p \leq 0.05$) decreased in the nanocomposite films containing

Table 1 Influence of variable MMT and chitosan concentration on moisture related attributed of the gluten protein based bionanocomposite films

Films	Moisture content (%)	Water activity	WAC (%)	Water solubility (%)	WVTR (g/h cm^2)
Control	$16.85^{a} \pm 0.01$	$0.55^{a} \pm 0.04$	$60.37^{a} \pm 0.07$	$34.84^{a} \pm 0.04$	$1.86^{a} \pm 0.07$
MC1	$15.12^{e} \pm 0.08$	$0.32^{b} \pm 0.05$	$41.15^{b} \pm 0.06$	$25.58^{b} \pm 0.07$	$0.16^{b} \pm 0.05$
MC2	$15.52^{d} \pm 0.02$	$0.40^{bc} \pm 0.04$	$36.88^{c} \pm 0.09$	$19.74^{c} \pm 0.08$	$0.06^{c} \pm 0.01$
MC3	$16.60^{c} \pm 0.01$	$0.26^{d} \pm 0.07$	$33.44^{d} \pm 0.04$	$18.83^{d} \pm 0.10$	$0.22^{b} \pm 0.06$
MC4	$16.69^{b} \pm 0.05$	$0.37^{b} \pm 0.07$	$28.20^{e} \pm 0.02$	$18.08^{e} \pm 0.08$	$0.14^{bc} \pm 0.06$

Control—gluten 5% + PVA 5%; MC1—MMT 2% + gluten 5% + PVA 5% + Chitosan 1.5%; MC2—MMT 2% + gluten 5% + PVA 5% + Chitosan 2.5%; MC3—MMT 4% + gluten 5% + PVA 5% + Chitosan 1.5%; MC4—MMT 4% + gluten 5% + PVA 5% + Chitosan 2.5%

MMT montmorillonite, *PVA* polyvinyl alcohol

*Results represent mean value of 3 results ± standard deviation. Values having different superscripts from a, b, c, d, and e are significantly ($p \leq 0.05$) different from each other when compared means through SPSS Statistics 20 Duncan's post hoc test

Table 2 Influence of variable MMT and chitosan concentration on mechanical properties and thickness of the gluten protein based bionanocomposite films

Sample	Tensile strength (MPa)	Elongation at break (%)	Thickness (mm)
Control	$18.71^{e} \pm 0.05$	$19.69^{c} \pm 0.81$	$0.12^{ab} \pm 0.01$
MC1	$37.57^{d} \pm 0.73$	$28.73^{a} \pm 0.61$	$0.15^{b} \pm 0.02$
MC2	$58.94^{a} \pm 0.08$	$23.27^{b} \pm 0.34$	$0.10^{a} \pm 0.01$
MC3	$42.79^{c} \pm 0.42$	$12.32^{d} \pm 0.21$	$0.25^{c} \pm 0.01$
MC4	$51.50^{b} \pm 0.92$	$11.22^{d} \pm 1.00$	$0.33^{d} \pm 0.06$

Control—Gluten 5% + PVA 5%; MC1− MMT 2% + gluten 5% + PVA 5% + Chitosan 1.5%; MC2—MMT 2% + gluten 5% + PVA 5% + Chitosan 2.5%; MC3—MMT 4% + gluten 5% + PVA 5% + Chitosan 1.5%; MC4—MMT 4% + gluten 5% + PVA 5% + Chitosan 2.5%

MMT montmorillonite, *PVA* polyvinyl alcohol

*Results represent mean value of 3 results ± standard deviation. Values having different superscripts from a, b, c, d, and e are significantly ($p \leq 0.05$) different from each other when compared means through SPSS Statistics 20 Duncan's post hoc test

2% MMT/1.5% chitosan and increased in 4% MMT containing films respectively (Table 2). The MMT exfoliates entrapped the polymer matrix and enhanced the thickness of films by increasing the layer-by-layer packing of the polymer granules [3]. The correlation given in Table 3 represented the positive correlation with the increase in MMT concentration. Similar results were studies by Thakur et al. [21] who concluded that granules of matrix compressed closer together and packed more tightly as a result of the MMT particles attaching themselves between the chitosan chains. It involves the initial production of a monolayer followed by the development of several layers until the maximum thickness is attained.

Mechanical properties

TS and EAB are considered the important mechanical properties of packaging industries and data is illustrated in Table 2. The packaging films must be strong and resistant to breakage to endure the mechanical shock of handling during production, transportation, and packaging. The highest TS of MC2 (58.94 MPa) was observed in comparison with other nanocomposite films. The TS was significantly ($p \leq 0.01$) affected by the synergistic combination of MMT and chitosan ($R = 0.978$). These results were supported by researchers with the analysis of PVA/chitosan-based composite films [14]. These outcomes might have shown that the incorporation of nanoparticles could enhance the mechanical properties of the films and demonstrate the efficiency of the strong interaction between the surface hydroxyl group of MMT and the functional groups of both polymers [23]. TS of the films with the concentration of MMT 4% was slightly reduced and torn off at a particular point with a constant force. High concentration of MMT enhanced thickness of the film due to multiple layers and the particles of the MMT aggregate to each other. Previous research has shown that MMT can agglomerate at higher polymer MMT levels (> 3%), which can reduce mechanical performance in comparison to lower MMT contents [18, 24]. Mahmoudian et al. [25], explained the good dispersion of MMT in cellulose and enhanced the tensile strength by up to 12%

EAB was independent of wheat gluten content and the preparatory method of films. Concerning the entire range of chitosan content (1.5–2.5%), the EAB reduced with the rise in chitosan content [12]. The combination with 2% MMT and 1.5% chitosan a showed higher EAB value (28.73%)

Table 3 Pearson's correlation coefficient between different variables of gluten-MMT based nanocomposite films

	MMT concentration	Chitosan concentration	Moisture content	Water activity	Thickness	Tensile strength	Elongation at break	Opacity	Antioxidant activity	Water solubility	WVTR	Water absorption capacity
MMT concentration	1	0.700	0.109	−0.823	0.460	0.657	−0.614	0.907*	0.688	−0.906*	−0.772	−0.939*
Chitosan concentration	0.700	1	−0.357	−0.549	−0.172	0.978**	−0.151	0.337	0.955**	−0.906*	−0.899*	−0.900*
Moisture content	0.109	−0.357	1	0.320	0.178	−0.353	−0.841	0.323	−0.203	0.143	0.524	0.148
Water activity	−0.823	−0.549	0.320	1	−0.666	0.531	0.155	−0.776	0.420	0.764	0.837	0.789
Thickness	0.460	−0.172	0.178	−0.666	1	−0.121	−0.327	0.698	−0.304	−0.235	0.836	−0.212
Tensile strength	0.657	0.978**	−0.353	−0.531	−0.121	1	−0.146	0.283	0.884*	−0.909*	−0.875*	−0.859
Elongation at break	−0.614	−0.151	−0.841	0.155	−0.327	−0.146	1	−0.693	−0.256	0.410	0.019	0.405
Opacity	0.907*	0.337	0.323	−0.776	0.698	0.283	−0.693	1	0.355	−0.655	−0.503	−0.712
Antioxidant activity	0.688	0.955**	−0.203	−0.420	−0.304	0.884*	−0.256	0.355	1	−0.828	−0.790	−0.866
Water solubility	−0.906*	−0.906*	0.143	0.764	−0.235	−0.909*	0.410	−0.655	−0.828	1	0.906*	0.978**
WVTR	−0.772	−0.899*	0.524	0.836	0.836	−0.875*	0.019	−0.503	−0.790	0.906*	1	0.917*
Water absorption capacity	−0.939*	−0.900*	0.148	0.789	−0.212	−0.859	0.405	−0.712	−0.866	0.978**	0.917*	1

*Correlation is significant at 0.05 level (2-tailed)

**Correlation is significant at 0.01 level (2-tailed)

and the film (MC2) consisting of 2.5% chitosan had a slight decrease in the EAB profile i.e., 23.27% (Table 2). Further, EAB reduced up to 11.22% with the increase in chitosan and MMT concentration in comparison with the control film. The change in concentrations of MMT and chitosan with the constant proportion of gluten/PVA has negatively correlated with the EAB property of films (Table 3). This might be explained by the presence of MMT, which prevents RC chains from slipping during deformation and reduces EAB values as a result [25]. Vahedikia et al. [8] also described that nanoparticle promoted the reducing trend of EAB with the increasing concentration of chitosan nanoparticles. The obtained results were also supported by Xu et al. [26] in starch nanocomposite films with the incorporation of cellulose nanocrystals at the level of 5% to 15%. However, Tunc et al. [6] found slight increase in EAB values of the gluten-based films with the MMT concentration of 2.5% and afterwards significant decrease in the EAB value of nanocomposite film had a concentration of MMT of more than 5%.

Morphological analysis

FE-SEM micrograph in Fig. 3, represents the surface and cross-sectional topography of various bionanocomposite films. It was illustrated that the control film (Fig. 3a) had multiple cracks appearing on the surface due to the brittleness of the films. This could be due to the large particles of gluten might affected by hydrophobic interactions and the pH of the blend [2]. Whereas, the addition of MMT and chitosan in combination with PVA and glycerol gave flexible, highly swellable smooth and firm topography. A high degree of exfoliation and intercalation was found in the films with 2% concentration of MMT (Fig. 3b, c). This could be a result of the multilayer silicates of MMT being exfoliated and evenly disseminated throughout the entire matrix of gluten, glycerol, PVA, and chitosan [27]. Another study also supported similar results in which The TiO2 NPs and ZEO were evenly distributed throughout the samples, which were shown on the SEM graphs to have a uniform and homogenous structure [13]. However, in Fig. 3d and e (MMT-4%) indicated irregularities, lumps and few cracks appeared due to less exfoliation of high concentration of MMT nanoclays. Furthermore, the agglomerates on the surface of films cause the formation of small cavities on the surface and lead to a reduction in TS, appearance, and enhancement of water transmission of the films [28].

XRD analysis

The dispersion condition of the nano clay (MMT) and chitosan in the polymer matrix of gluten and PVA is determined by XRD. This technique was used to examine the molecular crystallinity and purity of MMT and chitosan in gluten matrix. The gluten and PVA polymer units in the control film did not interact, thus preventing the formation of single-material crystal zones in each component [7]. However, Fig. 4 represented the XRD diffractogram of different films which represents the broad-spectrum peaks in the control

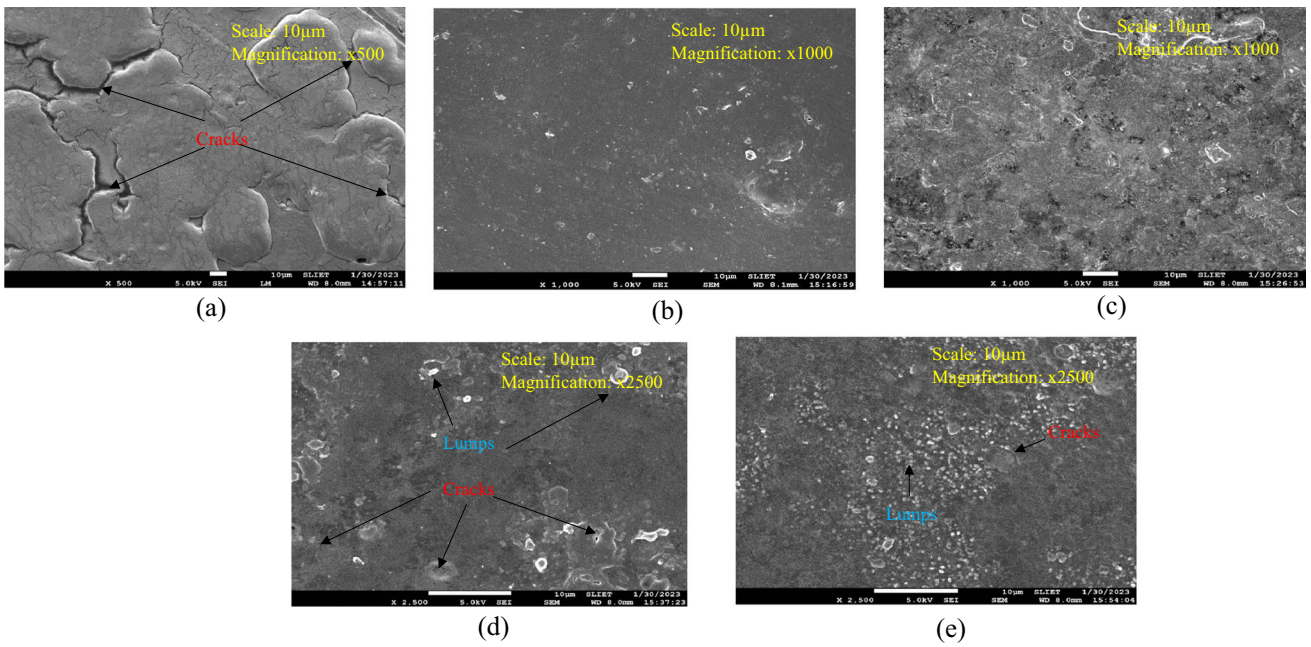

Fig. 3 FE-SEM micrograph of **a** gluten-PVA control film, **b** gluten/MMT-2%/chitosan 1.5% (MC1), **c** Gluten/MMT-2%/chitosan 2.5% (MC2) **d** gluten/MMT-4%/chitosan 1.5% (MC3) **e** gluten/MMT-4%/chitosan 2.5% (MC4)

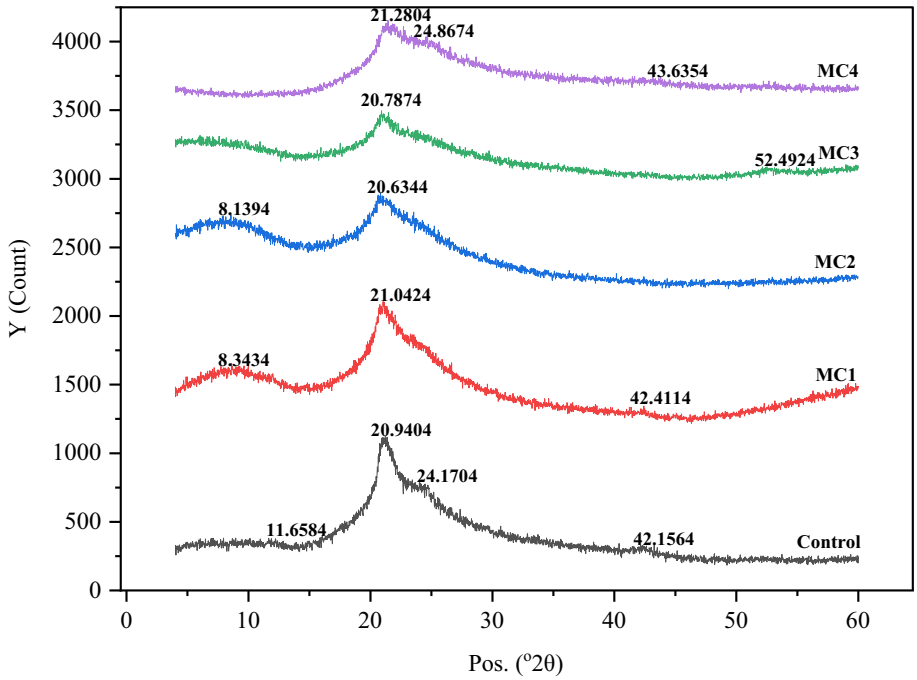

Fig. 4 XRD diffractogram of gluten based bionanocomposite films as Control (Gluten/PVA), Gluten/MMT-2%/chitosan 1.5% (MC1), Gluten/MMT-2%/chitosan 2.5% (MC2), Gluten/MMT-4%/chitosan 1.5% (MC3) and Gluten/MMT-4%/chitosan 2.5% (MC4)

film at 2Θ = 9° and 2Θ = 22° (black color pattern). Similarly, the incorporation of 2% MMT and 1.5% chitosan gave approximately the same characteristic peaks as 2Θ = 10° and 2Θ = 21° (Red color pattern). The crystallization peak intensity was highest in the control and the sample with 2% MMT and 1.5% chitosan. Whereas, a combination of MMT 2% and chitosan 2.5% illustrates a decrease in peak intensity to control film by increasing the chitosan concentration. The intermolecular interaction of exfoliated MMT and chitosan depicts the change in crystallographic profile. The MMT galleries absorbed and intercalated the PVA-gluten matrix uniformly and further changed their crystal configurations [29]. On the other hand, a slight decrease in the remaining two films with MMT 4% represented a doublet at 2Θ = 20° and 23° (green color pattern) and a distinguished peak at 22° and 25° (purple color pattern). The peaks were diffracted at lower area in MC2, MC3 and MC4 at 8.70° (d spacing = 1.15 Å), 20.87° (d spacing = 4.25 Å) and 22.38° (d spacing = 3.96 Å), respectively. Tetrahedral layers of silica and octahedral layers of alumina are sandwiched together to form the aluminum–silicate clay known as MMT. Chitosan chains that have been hydrated crystallize in an orthorhombic unit cell, which may be intercalated in exfoliated MMT galleries and in charge of moving the peaks to a lower level [21, 30]. The increase of inter sheet distance of 1.15–4.25 Å also represented the interaction of bilayers of chitosan with interlayers of MMT and the construction of intercalated structure [31]. A similar interpretation was illustrated by a study in which gluten and PVA were incorporated in nano clays for the development of nanocomposite films [32]. The observations lead to the crystallinity of the individual gluten and PVA polymers that is lower than that of the polymer composite containing MMT and chitosan.

Fourier transform infrared (FT-IR) analysis

The existence of particular functional groups in the molecular structure of polymers can be determined using FT-IR spectroscopy. These properties may be possessed by phase interactions and crystallinity between polymers and nano clays [3]. Figure 5 represented the FT-IR spectra with vibrational stretching and bending in different bionanocomposite films. Some of the distinctive peaks are observed and supported by the bands found in another research based on nanoparticles and organic polymer [13, 14]. In control and nanocomposite films, there were distinctive peaks between 922 to 1105/cm which represent the C–O–C stretching in PVA and Chitosan. The vibrations in ring and side functional groups may be the cause of the stretching and strong peaks of about 1100 cm [33]. In the present investigation, maximum stretching was observed in MMT at 1034/cm with the bending of Si–O–Si linkages [31]. Also, O–H bending was observed in PVA and polymer hydroxyl groups that produced hydrogen bonds [34]. The cluster of peaks around 1400/cm is due to multiple C–C stretching modes. The wide area of a band in the same region indicates a strong relationship between MMT and gluten matrix. It is possible to divide the amide band into its constituent parts based on the secondary structure of gluten and the aliphatic nitro compounds that represented the band region at wavenumber 1559/cm (60% N–H bending and 40% C–N stretching) [35]. Similarly, Arfat et al. [36] reported that the shift at amide

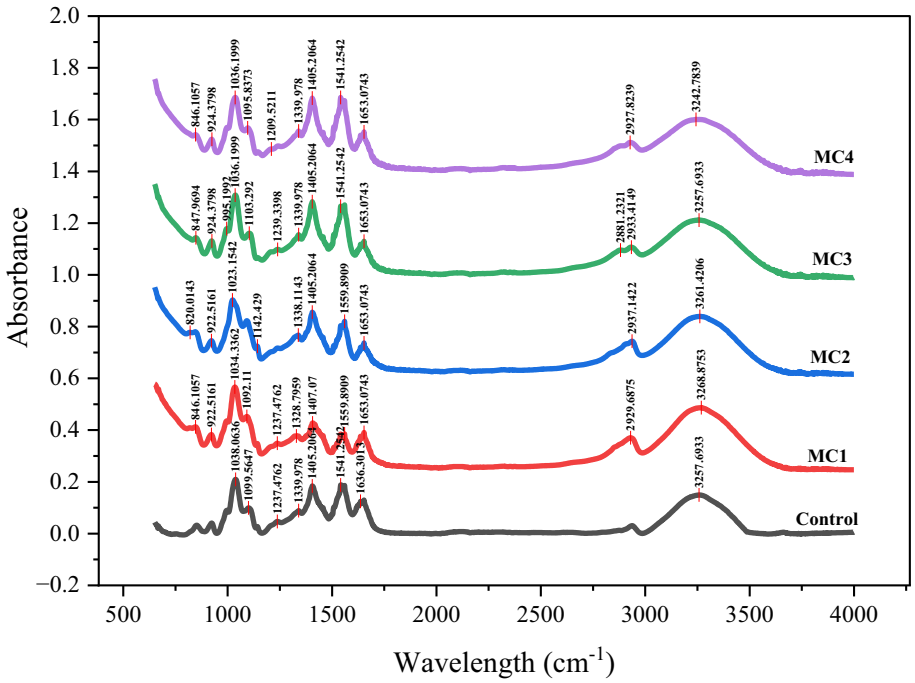

Fig. 5 FTIR spectra of gluten based bionanocomposite films as Control (Gluten/PVA), Gluten/MMT-2%/chitosan 1.5% (MC1), Gluten/MMT-2%/chitosan 2.5% (MC2), Gluten/MMT-4%/chitosan 1.5% (MC3) and Gluten/MMT-4%/chitosan 2.5% (MC4)

bands to a lower wavelength was observed to be generated by the addition of ZnO NPs to the fish protein isolate/fish skin gelatin-based composite films. Whereas, in control films, the wavenumber was shifted at 1541/cm (asymmetric stretching of aromatic compounds) which might be due to the reason that the amide band is sensitive to denaturation. The low-frequency peak with C=C stretching was found at 1653/cm in nanocomposite films. In some studies, the spectral region around 1660–1660 was found as nitrite (N=O) stretching [4, 37]. The low-intensity band region at 2927 to 2937/cm is illustrates the symmetric stretching of the C-H group. Further, gluten-based films depict a broad peak at the range of 3257 to 3268/cm with O–H stretching spectral region exhibiting moderate shifting trend towards lower wavenumber in contrast to control film. The prominent wide peak correlated with the O–H group that is involved in the production of hydrogen bonds. Shifting leads to the breakdown of hydrogen bonds within the gluten polymer results the increased interaction between MMT and gluten through their OH-group [13]. From the above results, the frequency of noticeable peaks after 1653/cm was reduced due to the interaction of the N–H group of gluten and the OH-group of chitosan [38]. As regards this study, the nanocomposite film with the concentration of 2% MMT and 2.5% chitosan (MC2) led to the best results of moisture barrier properties

Table 4 Influence of variable MMT and chitosan concentration on color properties, opacity and antioxidant activity of the gluten protein based bionanocomposite films

Sample	Color				Opacity ($AUmm^{-1}$)	Antioxidant activity (%)
	L*	a*	b*	ΔE		
Control	$87.56^{e} \pm 0.52$	$-0.89^{c} \pm 0.04$	$1.68^{c} \pm 0.07$	–	$2.37^{d} \pm 0.33$	$6.28^{e} \pm 0.04$
MC1	$84.81^{d} \pm 0.42$	$0.26^{a} \pm 0.08$	$3.32^{a} \pm 0.05$	$5.72^{a} \pm 2.45$	$3.08^{c} \pm 0.21$	$10.21^{c} \pm 0.10$
MC2	$78.54^{c} \pm 0.39$	$-1.05^{d} \pm 0.05$	$1.73^{c} \pm 0.03$	$9.11^{a} \pm 0.92$	$2.47^{d} \pm 0.23$	$12.53^{b} \pm 0.16$
MC3	$67.21^{b} \pm 0.10$	$-0.73^{b} \pm 0.05$	$2.81^{b} \pm 0.05$	$21.67^{b} \pm 0.74$	$4.30^{a} \pm 0.17$	$9.55^{d} \pm 0.55$
MC4	$64.57^{a} \pm 0.26$	$-0.85^{c} \pm 0.06$	$3.39^{a} \pm 0.11$	$25.93^{c} \pm 0.33$	$3.87^{b} \pm 0.11$	$14.81^{a} \pm 0.14$

Control—Gluten 5% + PVA 5%; MC1—MMT 2% + gluten 5% + PVA 5% + Chitosan 1.5%; MC2—MMT 2% + gluten 5% + PVA 5% + Chitosan 2.5%; MC3—MMT 4% + gluten 5% + PVA 5% + Chitosan 1.5%; MC4—MMT 4% + gluten 5% + PVA 5% + Chitosan 2.5%

L*—Lightness, a*—redness or greenness, b*—yellowness or blueness, ΔE—total color difference, MMT—Montmorillonite, PVA—polyvinyl alcohol

*Results represent mean value of 3 results ± standard deviation. Values having different superscripts from a, b, c, d, and e are significantly ($p \leq 0.05$) different from each other when compared means through SPSS Statistics 20 Duncan's post hoc test

and mechanical strength. This could be due to more attachment between functional groups of MMT and gluten.

Color

The visual appearance has a significant role in the consumer acceptability of biopolymeric films in the packaging of food items. Data illustrated in Table 4 as the values of lightness (L*), green–red (a*) and blue-yellow (b*) and total color difference (ΔE) of the developed nanocomposite films. The L* value of the control film was 87.56 which represents good transparency of the film. However, as the concentration of MMT and chitosan increased, the whiteness of the films decreased significantly ($p \leq 0.05$) from 84.81 (MC1) to 65.57 (MC4). This is due to the addition of MMT which gave a translucent appearance to the films. Due to the possibility that the hydroxyl group of chitosan could be well adsorbed with the exfoliates of MMT nano clay, the whiteness of MC2 was acceptable with a value of 78.54 [21]. Whereas, the enhanced concentration of MMT (4%) gave opaque and more thick films as supported by the FE-SEM images represented in Fig. 3. The high concentration of MMT enhanced greenish-blue color due to inadequate clay platelet exfoliation. The findings were in harmony with the results discussed by Gohargani et al. [17], concluded that nanoparticles may cause a loss in film transparency because of their tendency to aggregate and obstruct light transmission. Additionally, the PVA and MMT combination can operate as a focal point for light dispersion, amplifying light absorbance, and raising opacity when the MMT layers are unevenly distributed [19]. MMT is nearly green in colour, adding it to PVA films will change the colour of the films, as evidenced by the values of the films being noticeably different from one another and exhibiting green hue in the films containing 4% MMT. Theoretically, the transmission of light should be constant as long as MMT layers are evenly distributed throughout the PVA matrix because their thickness is less than 1 nm (lower than the visible light wave number) [39]. On the other hand, MC3 (MMT 2% and chitosan 2.5%) showed less yellow color (1.73) in comparison with the films containing 4% MMT and 2.5% chitosan (3.39) i.e., MC4. This significant difference between the films might be due to the interaction of MMT exfoliates with chitosan produce yellow color carbon by products during heating. The outcomes were in accordance with the study conducted by Lai et al. [10] where chitosan/MMT films were incorporated for the packaging of cherry tomatoes.

Opacity

The color parameters and transparency were critical properties of the films in packaging applications. A material with strong UV absorption capacity may be a choice for product packaging in which opacity might help in products longer shelf life. The non-uniformity in the blend of films could lead to affect optical properties [40]. Therefore, transmittance of the developed film was investigated within the range of 400 to 800 nm represented in Fig. 6. Results illustrated in Table 4 indicated that the opacity was significantly ($p \leq 0.05$) different from the control sample with the increase in concentration of MMT. The transmittance was significantly increased ($R = 0.907$) from 26.33 to 58.42% at 600 nm wavelength. The observed trend is explained by the fact that the material's opacity marginally rises with a higher load of nanoclays. Hematite (Fe_2O_3) was present in the clay's structure because of its capacity to block UV light. Light is absorbed by the Fe^{3+} octahedral-sheet electron structure in

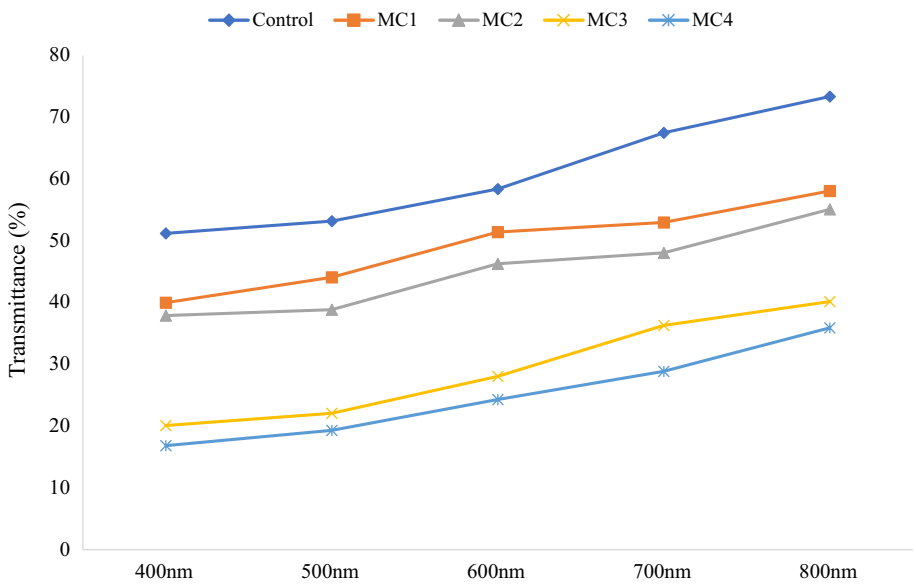

Fig. 6 Impact of different concentrations of variables MMT and chitosan on gluten based bionanocomposite films as Control (Gluten/PVA), Gluten/MMT-2%/chitosan 1.5% (MC1), Gluten/MMT-2%/chitosan 2.5% (MC2), Gluten/MMT-4%/chitosan 1.5% (MC3) and Gluten/MMT-4%/chitosan 2.5% (MC4)

MMT because it has an open orbital [41]. Some researchers found similar results, and reported that MMT increased the opacity of PVA films by reducing the transmission of visible light [15, 39]. Similarly, Tunc and Duman [42] found a reduction in the opacity of bionanofilms incorporated with variables cellulose and MMT. The opacity of control films (2.37) and MC2 (2.47) were non-significant to each other. MC2 represented more transparency and optimum color difference ($\Delta E = 9.11$) as compared to the other nanocomposite films. The MMT platelets were exfoliated through the gluten matrix in accordance with the XRD data, and their thickness of about 1 nm (less than the wavelength of visible light) which means they do not obstruct the flow of light. Additionally, chitosan and MMT interact each other through hydrogen bonding and improve optical properties at the concentration of 1.5% of chitosan and 2% of MMT. Opacity was slightly reduced with the increase in chitosan concentration from 1.5 to 2.5%. The results were supported by the scientific work related to chitosan-based bionanocomposite films with MMT nano clay conducted by Ramji and Vishnuvarthanan [43].

Water solubility (WS)

WS is an important parameter in the packaging material. The water resistance is correlated with the less WS of the packaging films. Data demonstrated in Table 1, indicated the significant ($p \leq 0.05$) decrease in WS ranged from 34.84 to 18.08%. This phenomenon is negatively correlated ($R = -0.906$) with the increasing concentration of MMT (2–4%) and chitosan (1.5–2.5%). The WS of control films was higher, given as 34.84% which is further decreased with the incorporation of MMT/chitosan in MC1, MC2, MC3 and MC4 by 26.58%, 43.34%, 45.95% and 48.11%. A similar decreasing trend was followed by Gujral et al. [20] in the starch-based nanocomposite films. The reduction in WS could be because of the increased amount of chitosan and MMT, which causes glycerol and other soluble (and hydrophilic) components to bind with them. This may be particularly true at the beginning of agglomeration and the creation of a distinct chitosan/MMT rich phase [4]. According to Abdollahi et al. [44], the crystalline index of the nanofillers decreased solubility through the improvement of the cohesiveness of the biopolymer matrix as a result of a hydrogen bond being formed between the gluten matrix and the hydroxyl groups of MMT by a dipole–dipole interaction. Some studies elaborated that the reduction of WS caused by the addition of PVA and crystalline nano-SiO_2 indicates that SiO_2 acts as a crystallisation aid and raises the degree of crystallinity in the polymer matrix [14, 19]. Similar results were discussed by Voon et al. [45] in gelatin films containing an increasing trend of nano clays. Nanocomposite films. A crucial component of biodegradable films is water insolubility, which has various advantages for usage as biomaterial devices. Additionally, Table 3 indicated the negative correlation of TS with WS. This might be due to more interlayer adhesion between the nanofillers and matrix causing high TS and low WS which do not allow its interaction with the matrix [46].

Water absorption capacity (WAC)

Gluten possesses strong water absorption property and needs to be resolved in order to use protein materials in packaging. Therefore, cross-linking agents and plasticizers play an important role in the modification of such material [4]. WAC of the developed films is given in Table 1. WAC of the control film was found highest (60.37%) and further reduction was found in the nanocomposite films containing nano clay and chitosan. The WAC property was significantly ($p \leq 0.05$) altered from 31.84 to 53.29% in comparison with the control film. In a similar manner to WS, WAC was found as negatively correlated with the concentration of MMT ($R = -0.939$) and chitosan ($R = -0.900$). WS and WAC are positively correlated ($R = 0.978$) to each other as both increased in a similar trend. According to the above-mentioned experimental results the polymer matrix makes strong hydrogen bonds with the exfoliated MMT. Therefore, free water molecules do not interact with nanocomposite films (gluten/PVA/MMT) as strongly as they do with composite films (gluten/PVA) alone [42]. The findings are not only consistent with the results of WS as well as outcomes on nanocomposites reported by other researchers [47, 48]. WAC has direct positive correlation with WVTR at the significance level of 0.05 ($R = 0.917$). The significant decrease in WAC could be due to the adhesive property of PVA within the gluten and MMT matrix which make strong crosslink junctions in the matrix [45, 49]. Souza et al. [50] studied the WAC of chitosan/MMT nanocomposite films and discussed a slight reduction in WAC properties with an increase in MMT concentration. In order to minimize early moisture-related failures, it is crucial to understand how polymeric materials behave both during processing such as during solution casting and in damp or humid conditions.

Water vapor transmission rate (WVTR)

WVTR is a crucial factor in food packaging that pertains to the transfer of moisture between food and the environment. A film's capacity to resist moisture is a crucial quality in packaging applications, especially when food items are being stored [51]. The WVTR of the control and nanocomposite films is represented in Table 1. WVTR value of control film is 1.86 g/h cm^2 and significantly ($p \leq 0.05$) reduced with the incorporation of MMT and chitosan in MC2 and MC3 as 0.16 g/h cm^2 and 0.06 g/h cm^2. Similar outcomes

were observed in research on potato starch-based nanofiber films. The decrease in WVTR with increasing MMT loading may be related to the establishment of hydrophilic interactions between gluten proteins and nano clays which resulted in lower availability of the hydrophilic sites for water vapor [52]. Several variables could influence the water vapor permeability of films, such as the molecular weight of the polymers, the type and degree of crosslinking, and the preparation circumstances, which would alter the network structure in polymeric films [15]. According to Calambas et al. [40], the increased crosslinking between the polymer matrix and nano clay suggests that polymeric chains acquire compactness over time, reducing interstitial gaps in the matrix and enabling a slower rate of water diffusion across the chain. Furthermore, an increase in MMT concentration of around 4%, enhanced the WVTR value in MC3 (0.22 g/h cm^2) and MC4 (0.14 g/h cm^2). WVTR of the nanocomposite films is negatively correlated with MMT ($R = -0.772$) and chitosan concentration ($R = -0.900$). Similar findings were noticed by Hassannia-Kolaee et al. [53] incorporated the MMT concentration from 1 to 5%, results a decrease in WVTR up to 3% due to the enhancement of tortuous and layered configuration of MMT exfoliates. Whereas, film containing 5% MMT level had a significant reduction could be due to multiple cracks that appeared as identified in the FE-SEM micrographs (Fig. 3d, e) of the film may allow free water to pass through the film.

Antioxidant activity

Oxidation is one of the primary reasons for food spoilage which occurs when oxygen comes into contact with components like fat or pigments [52]. Estimation was done by using the DPPH technique to confirm free radical scavenging due to the presence of antioxidant properties of all composite films (Table 4). Films made with gluten/MMT/chitosan had antioxidant activities that were noticeably higher than those of the control. As expected, the control film displayed the lowest antioxidant activity of 6.28%. Whereas, the increase in chitosan significantly ($p \leq 0.01$) increased the antioxidant activity of nanocomposite films. It is positively correlated ($R = 0.955$) with the increase in concentration of chitosan. The antioxidant activity of MC1 (10.21%) and MC2 (12.53%) was increased to 62.57% and 99.52%, respectively in comparison to control film. Similar, studies were observed by Jakubowska et al. [54], in which the different concentration of chitosan and plasticizer in the packaging film were used. Chitosan's antioxidant action is typically linked to its effectiveness at chelating metal ions, as this slows the start of lipid oxidation, functioning as a secondary antioxidant [55]. Moreover, chitosan films and coatings have low oxygen permeability, which slows the speed of oxidation of packed foods by simply avoiding their contact with oxygen [56]. Furthermore, the change in MMT concentration has a negligible effect on the antioxidant profile as investigated by Alexandre et al. [57] in the gelatin/MMT based nanocomposite packaging films.

Soil burial test

The significant degradation of nanocomposite films along with control film was illustrated in the form of weight loss during weekly intervals of time (Table 5). Enzymes and microorganisms play an important role in the biodegradation of the films. Enzymes can occur under aerobic and anaerobic circumstances and promote molecular breakdown, which can lead to partial or complete degradation from the environment [20]. Figure 7 represented the soil burial (55 days) of control and nanocomposite films. The control film contains gluten with disulfide bonds when under moist conditions comes in contact with enzymes and gram-negative bacteria that could easily degrade the film [58]. The degradation period of MMT-reinforced films was 14 days over the degradation period of control films. This interprets that control films

Table 5 Effect of variables MMT and chitosan on the weight loss profile under soil for biodegradability of films during specific intervals of time

Films	Time intervals (days)							
	Day 7	Day 14	Day 21	Day 28	Day 35	Day 41	Day 48	Day 55
Control	$15.32^{d} \pm 0.13$	$26.44^{e} \pm 0.03$	$43.71^{e} \pm 0.18$	$55.16^{e} \pm 0.12$	$79.47^{d} \pm 0.07$	$88.22^{c} \pm 0.09$	$98.84^{d} \pm 0.17$	–
MC1	$11.42^{e} \pm 0.09$	$21.34^{d} \pm 0.58$	$38.56^{d} \pm 0.35$	$49.45^{d} \pm 0.53$	$73.53^{c} \pm 0.12$	$88.42^{c} \pm 0.07$	$96.34^{c} \pm 0.29$	$99.01^{c} \pm 0.10$
MC2	$6.54^{b} \pm 0.11$	$11.61^{b} \pm 0.05$	$32.45^{c} \pm 0.17$	$48.91^{c} \pm 0.13$	$73.32^{c} \pm 0.13$	$89.39^{d} \pm 0.09$	$96.21^{c} \pm 0.15$	$98.04^{b} \pm 0.07$
MC3	$8.90^{c} \pm 0.05$	$17.52^{c} \pm 0.12$	$29.40^{b} \pm 0.23$	$42.20^{b} \pm 0.09$	$68.5^{b} \pm 0.06$	$80.03^{b} \pm 0.19$	$92.00^{b} \pm 0.27$	$97.93^{b} \pm 0.04$
MC4	$2.51^{a} \pm 0.10$	$6.91^{a} \pm 0.11$	$20.50^{a} \pm 0.09$	$29.80^{a} \pm 0.14$	$40.5^{a} \pm 0.20$	$67.40^{a} \pm 0.22$	$80.21^{a} \pm 0.091$	$96.72^{a} \pm 0.21$

Control—Gluten 5% + PVA 5%; MC1—MMT 2% + gluten 5% + PVA 5% + Chitosan 1.5%; MC2—MMT 2% + gluten 5% + PVA 5% + Chitosan 2.5%; MC3—MMT 4% + gluten 5% + PVA 5% + Chitosan 1.5%; MC4—MMT 4% + gluten 5% + PVA 5% + Chitosan 2.5%

MMT montmorillonite, *PVA* polyvinyl alcohol

*Results represent mean value of 3 results ± standard deviation. Values having different superscripts from a, b, c, d, and e are significantly ($p \leq 0.05$) different from each other when compared means through SPSS Statistics 20 Duncan's post hoc test

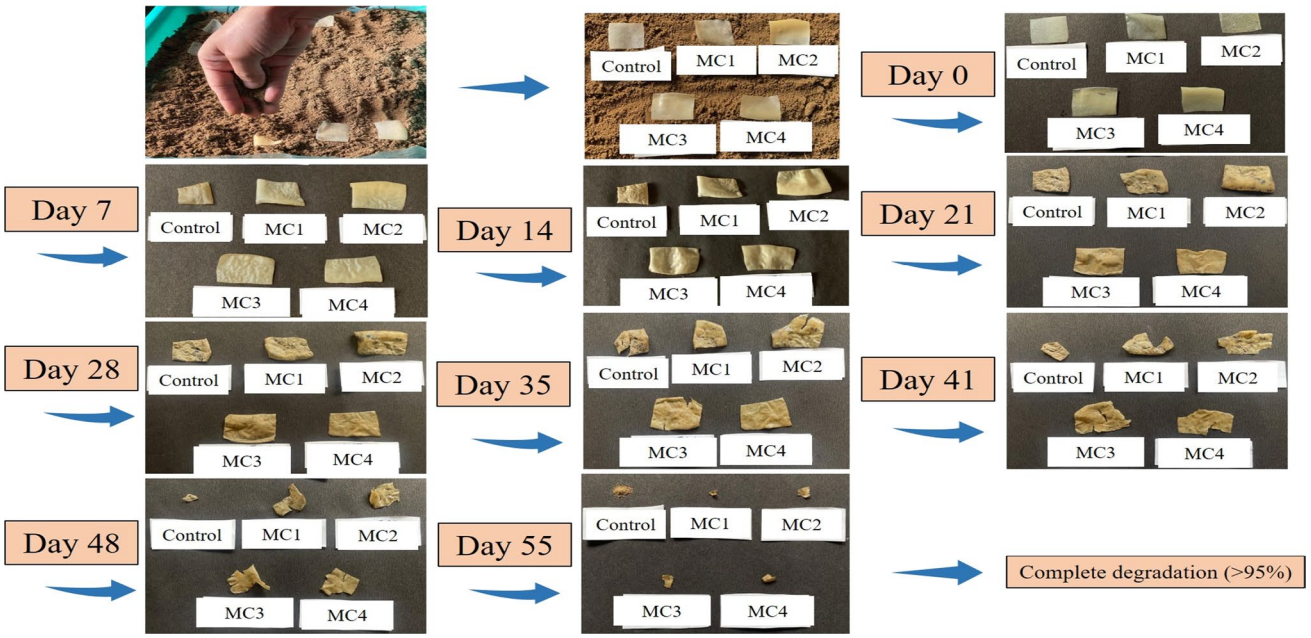

Fig. 7 Influence of environmental factors on the weight and appearance of the bionanocomposite films as Control (Gluten/PVA), Gluten/MMT-2%/chitosan 1.5% (MC1), Gluten/MMT-2%/chitosan 2.5% (MC2), Gluten/MMT-4%/chitosan 1.5% (MC3) and Gluten/MMT-4%/chitosan 2.5% (MC4) under a specific intervals of day

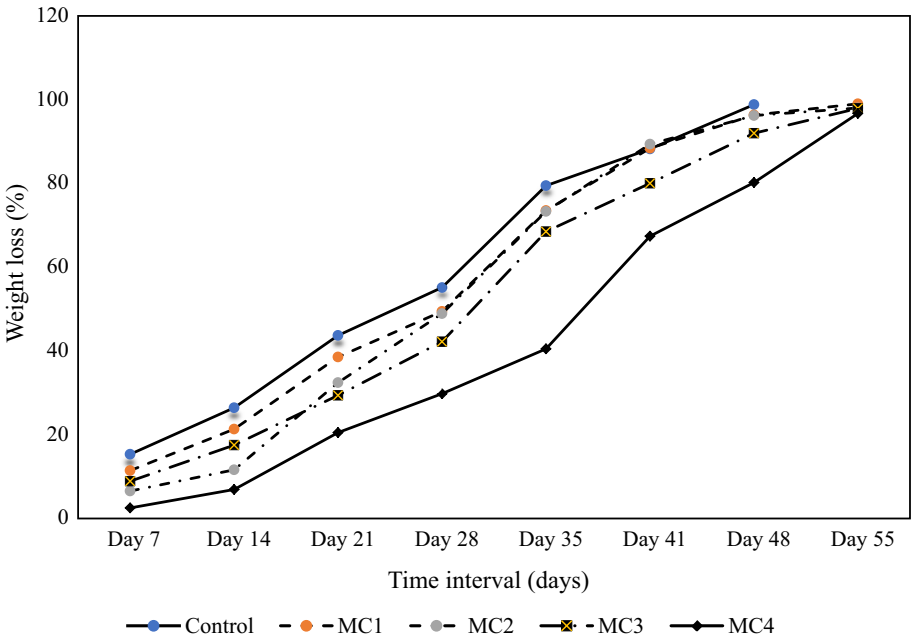

Fig. 8 Impact on soil degradation of gluten-based films formulated with different nanoparticles and antimicrobial agents i.e., Control (Gluten/PVA), Gluten/MMT-2%/chitosan 1.5% (MC1), Gluten/MMT-2%/chitosan 2.5% (MC2), Gluten/MMT-4%/chitosan 1.5% (MC3) and Gluten/MMT-4%/chitosan 2.5% (MC4)

almost completely degraded within 48 days whereas nanocomposite films took more than 55 days for maximum degradation. The weight loss in MC1 (38.6%) and MC3 (29.4%) during day 21 was very rapid, whereas degradation of MC2 (48.9%) and MC4 (29.8%) was rapid till day 28 under conditioned soil (Fig. 8). The poor dispersion of MMT and gluten matrix could lead to failure in physical compactness of the composite because of stress points created in the films. It is possible that the addition of MMT significantly slowed the biodegradation of the films, this is because these films have MMT layers inside of them, which act as a barrier and reduce the amount of water that can diffuse into the films, causing this effect. The hydroxyl group (OH-) of MMT tends to make strong hydrogen interactions with the hydroxyl group (OH-) of chitosan, which improves the interaction of the molecules and ultimately increases the cohesiveness of the film and

decreases weight loss [13]. These results were in agreement with those reported by Gujral et al. [20], who discussed that native maize starch-based films degrade more quickly than nanoparticle-reinforced films. Additionally, the increase in chitosan also significantly affected the degradation rate of the films because of its interaction with gluten/PVA form compact matrix and exerts antimicrobial properties [59]. Oyeoka et al. [50] interpret the results related to soil degradation of PVA/gelatin-based films and gave reason that due to moisture dispersion into the films causes film swelling and promotes microbial development, and subsequently due to enzymatic and other released degradation disrupting the film and causing weight loss. In another study, 95.93–98.11% degradation of films was observed in the starch-based composite films [48]. The previous studies and present scientific work could extract the stable films that were developed by the incorporation of nanoparticles which can hold the easily degradable polymer structure without hindering its mechanical strength.

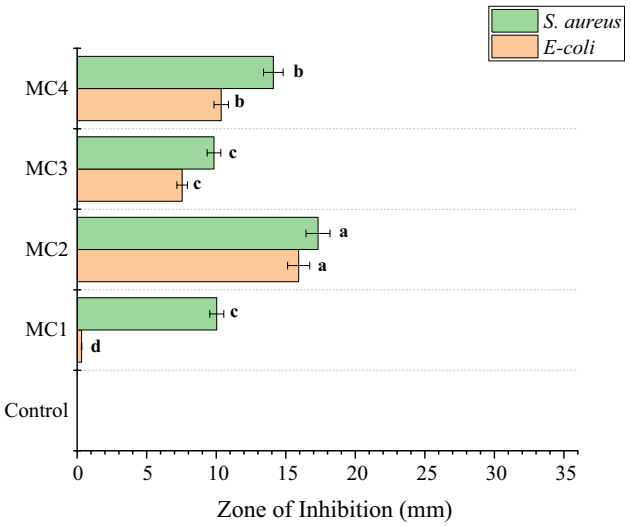

Fig. 9 Antimicrobial activity of the nanocomposite films as Control (Gluten/PVA), Gluten/MMT-2%/chitosan 1.5% (MC1), Gluten/MMT-2%/chitosan 2.5% (MC2), Gluten/MMT-4%/chitosan 1.5% (MC3) and Gluten/MMT-4%/chitosan 2.5% (MC4) against bacterial cultures of *Staphylococcus aureus* and *Escherichia coli*

Antimicrobial activity

The outcomes of antibacterial property against gram-positive (*S. aureus*) and Gram-negative (*E. coli*) bacteria of gluten films blended with MMT and chitosan are displayed in Fig. 9. The neat chitosan control films prepared of gluten and PVA has negligible antibacterial activity against both bacteria. The results indicated that nanocomposite films reinforced with MMT/chitosan exhibited good microbial inhibition zone against *S. aureus* (Fig. 10a) and *E. coli* (Fig. 10b). The inhibition possessed by MC2 and MC4 (chitosan 2.5%) was higher in comparison to MC1 and MC3 (chitosan 1.5%). Although, change in MMT nano clays does not possess any antimicrobial potential, alteration in the chitosan proportion causes an increase in the zone of inhibition (ZOI) [13]. This is a result of chitosan's inherent antibacterial activity, which involves binding positively charged chitosan amino groups to the primarily anionic components of the bacteria's cell surface [60]. The largest ZOI against *S. aureus* was found in the film sample MC2 (17.31 mm) followed by MC4 (14.11 mm), MC1 (10.04 mm) and MC3 (9.84 mm). A similar order of zone was obtained against *E. coli* with the largest ZOI indicated by MC2 (15.93 mm) followed by MC4 (10.36 mm), MC3 (7.55 mm) and MC1 (0.32 mm). Another important point is that the antimicrobial activity of the nanocomposite films against *S. aureus* was higher as compared to *E. coli*. This finding can be further explained by the structural differences between the outer membranes of Gram-positive and Gram-negative bacteria. Also, Gram-negative bacteria are more resistant to generated reactive oxygen species by chitosan due to their more complex cell wall construction, which consists of

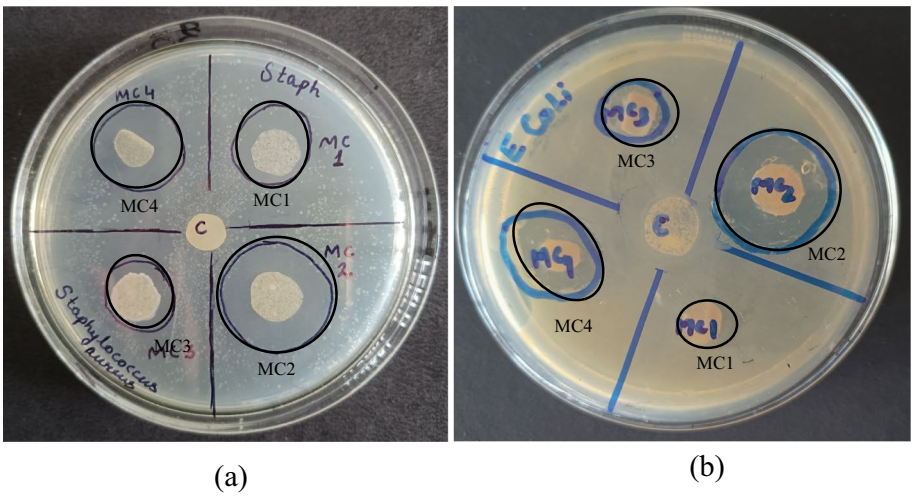

Fig. 10 Influence of variables including MMT and chitosan on the antimicrobial property of bionanocomposite film against bacterial i.e. **a** *Staphylococcus aureus*, **b** *E. coli*

a thin peptidoglycan layer and an outer membrane [61]. Moreover, similar findings were made in earlier research, which found that the antibacterial activity of AgNPs [62] and ZnONPs [63] integrated chitosan films were higher against gram-positive bacteria than against Gram-negative bacteria. In a comparable work, the antibacterial activity of chitosan-based film impregnated with modified MMT, nanosilver and silver zeolite had a positive inhibitory effect on the activity of *E. coli* [64]. It can be concluded that the synergistic effect of chitosan and nanoclays can increase the reduction of microbial count in more than one log cycle [13].

Conclusion

The nanocomposite films were successfully synthesized by using the solution casting method in which chitosan was used for the immobilization of MMT. The present study intimated changes in physicochemical attributes of the gluten/PVA based bionanocomposite films modified with different concentrations of MMT (2% and 4%) and chitosan (1.5% and 2.5%). The complex interaction of MMT and chitosan with the gluten/PVA matrix reduced the WAC and WS of the films. Also, WVTR was dependent on the uniform cross-links of the gluten-PVA matrix with MMT exfoliates. The increasing proportion of MMT produced darker films that is directly proportional to the opacity and thickness of the films. Further, the opacity and thickness of the films were found minimum in MC2 (MMT 2% + chitosan 2.5%) due to their molecular compatibility at similar proportions. Additionally, this compatibility produced negligible cracks on the surface of the films, whereas beyond that cracks drastically appeared as depicted by FE-SEM and XRD outcomes leading to water transmission and breakage of the films. On the other hand, mechanical properties like TS and EAB were comparatively higher and parallel to the plastic films in the market which must be an appreciable outcome of the research. Contrarily, the FT-IR spectrum also represented the interaction of multiple bonds with the nano clay and matrix. Furthermore, biodegradability as an ecofriendly factor was obtained more than 95% degradation within 55 days under soil conditions. The antimicrobial property was enhanced by chitosan as MC2 gave a maximum inhibition zone of 15.93 mm and 17.31 mm against *E. coli* and *S. aureus*, respectively. Conclusively, the films with 2% MMT and 2.5% chitosan (MC2) have comparatively better mechanical strength, high transparency, lowest water vapor transmission rate, low water activity, lower solubility, antimicrobial properties and cavity-free surface of the films and hence optimized for further modifications developed bionanocomposite films biodegradable and found very strong compared to plastic packaging, could be utilized as packaging material for perishable products i.e., dairy, meat, fruits, and vegetables, etc. However, in the future more detailed experiments should be performed in regards to the primary contact with the food and changes in its quality during storage for a longer time.

References

1. K. Deepika, P.L. Praveena, G. Srisugamathi, J. NilofarNisha, Mater. Today (2020). https://doi.org/10.1016/j.matpr.2020.02.389
2. J. Xu, Y. Li, J. Food Sci. **88**, 582–594 (2023). https://doi.org/10.1111/1750-3841.16454
3. F. Rafieiana, M. Shahedi, J. Keramat, J. Simonsen, Ind. Crops Prod. **53**, 282–288 (2014). https://doi.org/10.1016/j.indcrop.2013.12.016
4. M. Dabbaghianamiri, E.M. Duraia, G.W. Beall, J. Mater. Sci. (2020). https://doi.org/10.1016/j.rinma.2020.100101
5. J.M. Kim, M.H. Lee, J.A. Ko, D.H. Kang, H. Bae, H.J. Park, Food Sci. **83**, 349–357 (2018)
6. S. Tunc, H. Angellier, Y. Cahyana, P. Chalier, N. Gontard, E. Gastaldi, J. Membr. Sci. **289**, 159–168 (2007). https://doi.org/10.1016/j.memsci.2006.11.050
7. M. Pang, L. Cao, Y.S.H. Wang, CYTA. J. Food **17**, 400–407 (2019). https://doi.org/10.1080/19476337.2019.1587517
8. N. Vahedikia, F. Garavand, B. Tajeddin, I. Cacciotti, S.M. Jafari, T. Omidi, Z. Zahedi, Colloids Surf. B (2019). https://doi.org/10.1016/j.colsurfb.2019.01.045
9. M.R. Martelli, T.T. Barros, M.R. de Moura, L.H. Mattoso, O.B. Assis, J. Food Sci. **78**, 98–104 (2013)
10. Y. Lai, W. Wang, J. Zhao, S. Tu, Y. Yin, L. Ye, Food Packag. Shelf Life **33**, 100879 (2022)
11. A. Jokar, M.H. Azizi, Z.H. Esfehani, Nutr. Food Sci. **4**, 25–34 (2017)
12. F. Chen, X. Monnier, M. Gallstedt, U.W. Gedde, M.S. Hedenqvist, Eur. Polym. J. **60**, 186–197 (2014). https://doi.org/10.1016/j.europolymj.2014.09.007
13. P. Singh, G. Kaur, A. Singh, P. Kaur, J. Food Meas. Charact. (2022). https://doi.org/10.1007/s11694-022-01635-4
14. M. Kariminejad, R. Zibaei, A. Kolahdouz-Nasiri, R. Mohammadi, A.M. Mortazavian, S. Sohrabvandi, E. Khanniri, N. Khorshidian, Biointerface Res. Appl. Chem. **12**, 3725–3734 (2022). https://doi.org/10.33263/BRIAC123.37253734
15. S. Ahmed, S. Ikram, J. Photochem. Photobiol. B (2016). https://doi.org/10.1016/j.jphotobiol.2016.08.023
16. N. Benbettaieb, R. Mahfoudh, Int. J. Biol. Macromol. (2020). https://doi.org/10.1016/j.ijbiomac.2020.05.199
17. M. Gohargani, H. Lashkari, A. Shirazinejad, J. Food Qual. (2020). https://doi.org/10.1155/2020/8844167
18. A.A. Kadam, S. Singh, K.K. Gaikwad, Food Control (2021). https://doi.org/10.1016/j.foodcont.2021.107877
19. M. Kariminejad, E. Sadeghi, M. Rouhi, R. Mohammadi, F. Askari, M. Taghizadeh, S. Moradi, J. Food Process. Eng. (2018). https://doi.org/10.1111/jfpe.12817
20. H. Gujral, A. Sinhmar, M. Nehra, V. Nain, R. Thory, A.K. Pathera, P. Chavan, Int. J. Biol. Macromol. **186**, 155–162 (2021). https://doi.org/10.1016/j.ijbiomac.2021.07.005
21. G. Thakur, A. Singh, I. Singh, Sci. Pharm. **84**, 603–617 (2016). https://doi.org/10.3390/scipharm84040603
22. C.A. Gomez-Aldapa, G. Velazquez, M.C. Gutierrez, E. Rangel-Vargas, J. Castro-Rosas, R.Y. Aguirre-Loredo, Mater. Chem. Phys. (2020). https://doi.org/10.1016/j.matchemphys.2019.122027
23. W. Wang, H. Zhang, Y. Dai, H. Hou, H. Dong, Iran Polym. J. **24**, 687–696 (2015). https://doi.org/10.1007/s13726-015-0359-7

24. J. Lee, Q. Sun, Y. Deng, J. Biobased Mater. Bioenergy **2**, 162–168 (2008)
25. S. Mahmoudiana, M.U. Wahit, A.F. Ismail, A.A. Yussuf, Carbohydr. Polym. **88**, 1251–1257 (2012). https://doi.org/10.1016/j.carbpol.2012.01.088
26. Y. Xu, A. Scales, K. Jordan, C. Kim, E. Sismour, J. Appl. Polym. Sci. (2017). https://doi.org/10.1002/APP.44438
27. N.A. Negm, G.H. Sayed, F.Z. Yehia, O.I.H. Dimitry, A.M. Rabie, E.A.M. Azmy, Egypt J. Chem. **59**, 1045–1060 (2016)
28. I. Echeverría, P. Eisenberg, A.N. Mauri, J. Membr. Sci. **449**, 15–26 (2014). https://doi.org/10.1016/j.memsci.2013.08.006
29. A. García-Padilla, M.A.M.K. Moreno-Sader, A.R. Jimenez, J.B. Soares, Contemp. Eng. Sci. **11**, 1633–1641 (2018)
30. V.G.L. Souza, J.R.A. Pires, C. Rodrigues, P.F. Rodrigues, A. Lopes, R.J. Silva, J. Caldeira, M.P. Duarte, F.B. Fernandes, I.M. Coelhoso, A.L. Fernando, Coatings (2019). https://doi.org/10.3390/coatings9110700
31. O. Faruk, L.M. Matuana, Composite Sci. Technol. **68**, 2073–2077 (2008)
32. D.B. Lee, D.W. Kim, Y. Shchipunovc, C. Ha, Polym. Int. (2016). https://doi.org/10.1002/pi.5148
33. M. Fan, D. Dai, B. Huang, Fourier Transform—Materials Analysis. In Tech, London
34. S. Pawde, K. Deshmukh, J. Appl. Polym. Sci. **109**, 3431–3437 (2008). https://doi.org/10.1002/app.28454
35. S. Liang, Q. Huang, L. Liu, K.L. Yam, Macromol. Chem. Phys. **210**, 832–839 (2009). https://doi.org/10.1002/macp.200900053
36. Y.A. Arfat, S. Benjakul, T. Prodpran, P. Sumpavapol, Food Hydrocoll. **41**, 265–273 (2014). https://doi.org/10.1016/j.foodhyd.2014.04.023
37. L. Qu, G. Chen, S. Dong, Ind. Crops Prod. **130**, 450–458 (2019). https://doi.org/10.1016/j.indcrop.2018.12.093
38. R. Mohammadi, M.A. Mohammadifar, M. Rouhi, M. Kariminejad, A.M. Mortazavian, E. Sadeghi, S. Hasanvand, Int. J. Biol. Macromol. **107**, 406–412 (2018). https://doi.org/10.1016/j.ijbiomac.2017.09.003
39. G. Liu, Y. Song, J. Wang, H. Zhuang, L. Ma, C. Li, LWT Food Sci. Technol. **57**, 562–568 (2014)
40. H.L. Calambas, A. Fonseca, D. Adames, Y. Aguirre-Loredo, C. Caicedo, Molecules (2021). https://doi.org/10.3390/molecules26216734
41. S.A. Oleyaei, H. Almasi, B. Ghanbarzadeh, A.A. Moayedi, Carbohydr. Polym. (2016). https://doi.org/10.1016/j.carbpol.2016.07.040
42. S. Tunç, O. Duman, Appl. Clay Sci. **48**, 414–424 (2010). https://doi.org/10.1016/j.clay.2010.01.016
43. V. Ramji, M. Vishnuvarthanan, SILICON **14**, 1209–1220 (2022). https://doi.org/10.1007/s12633-021-01045-z
44. M. Abdollahi, M. Alboofetileh, R. Behrooz, M. Rezaei, R. Miraki, Int. J. Biol. Macromol. **54**, 166–173 (2013)
45. H.C. Voon, R. Bhat, A.M. Easa, M. Liong, A. Karim, Food Bioprocess Technol. **5**, 1766–1774 (2012). https://doi.org/10.1007/s11947-010-0461-y
46. A.E. Saputri, D. Praseptiangga, E. Rochima, C. Panatarani, I.M. Joni, in AIP Conference Proceedings, (AIP Publishing LLC 2018) p. 1927. https://doi.org/10.1063/1.5021233
47. F. Sadegh-Hassani, A.M. Nafchi, Int. J. Biol. Macromol **67**, 458–462 (2014)
48. A.R. Tawakaltu, E.C. Egwim, S.S. Ochigbo, P.C. Ossai, J. Mater, Sci. Eng. **5**, 372–379 (2015). https://doi.org/10.17265/2161-6221/2015.9-10.005
49. N. Jain, V.K. Singh, S. Chauhan, J. Mech. Behav. Mater. (2018). https://doi.org/10.1515/jmbm-2017-0027
50. H.C. Oyeoka, C.M. Ewulonua, I.C. Nwuzor, C.M. Obele, J.T. Nwabanne, J. Bioresour. Bioprod. (2021). https://doi.org/10.1016/j.jobab.2021.02.009
51. H. Bai, Y. Sun, J. Xu, W. Dong, X. Liu, Carbohydr. Polym. **115**, 422–431 (2015). https://doi.org/10.1016/j.carbpol.2014.08.103
52. E. Choe, D.B. Min, Compr. Rev. Food Sci. Food Saf. **8**, 345–358 (2015). https://doi.org/10.1111/j.1541-4337.2009.00085.x
53. M. Hassannia-Kolaee, F. Khodaiyan, I. Shahabi-Ghahfarrokhi, J. Food Sci. Technol. (2015). https://doi.org/10.1007/s13197-015-1778-3
54. E. Jakubowska, M. Gierszewska, J. Nowaczyk, E. Olewnik-Kruszkowska, Carbohydr. Polym. (2021). https://doi.org/10.1016/j.carbpol.2020.117527
55. S.B. Schreiber, J.J. Bozell, D.G. Hayes, S. Zivanovic, Food Hydrocoll. **33**, 207–214 (2013). https://doi.org/10.1016/j.foodhyd.2013.03.006
56. D. Georgantelis, I. Ambrosiadis, P. Katikou, G. Blekas, S.A. Georgakis, Meat Sci. **76**, 172–181 (2007)
57. E.M.C. Alexandre, R.V. Lourenço, A.M.Q.B. Bittante, I.C.F. Moraes, P.J.A. Sobral, Food Packag. Shelf Life **10**, 87–96 (2016). https://doi.org/10.1016/j.fpsl.2016.10.004
58. V. Koiv, T. Tenson, Appl. Microbiol. Biotechnol. **105**, 3045–3059 (2021). https://doi.org/10.1007/s00253-021-11263-5
59. R. Priyadarshi, J. Rhim, Innov. Food Sci. Emerg. Technol. **62**, 102346 (2020)
60. S.A. Marand, H. Almasi, N.A. Marand, Int. J. Biol. Macromol. **190**, 667–678 (2021). https://doi.org/10.1016/j.ijbiomac.2021.09.024
61. S. Amjadi, H. Almasi, M. Ghorbani, S. Ramazani, Food Packag. Shelf Life **24**, 100504 (2020). https://doi.org/10.1016/j.fpsl.2020.100504
62. A. Shah, M.A. Yameen, N. Fatima, G. Murtaza, Int. J. Pharm. **561**, 19–34 (2019). https://doi.org/10.1016/j.ijpharm.2019.02.029
63. J. Kaur, K. Sood, N. Bhardwaj, S.K. Arya, M. Khatri, Mater. Today Proc. **28**, 1904–1909 (2020). https://doi.org/10.1016/j.matpr.2020.05.309
64. J. Rhim, S. Hong, H. Park, K.W.N.G. Perry, J. Agric. Food Chem. **54**, 5814–5822 (2006). https://doi.org/10.1021/jf060658h